A New Hybrid-Mixed Composite Laminated Curved Beam Element

Ho-Cheol Lee, Jin-Gon Kim*

School of Mechanical & Automotive Engineering, Catholic University of Daegu, Hayang-up, Kyongsan-si, Kyongbuk, 712-702, Korea

In this study, we present a new efficient hybrid-mixed composite laminated curved beam element. The present element, which is based on the Hellinger-Reissner variational principle and the first-order shear deformation lamination theory, employs consistent stress parameters corresponding to cubic displacement polynomials with additional nodeless degrees in order to resolve the numerical difficulties due to the spurious constraints. The stress parameters are eliminated and the nodeless degrees are condensed out to obtain the (6×6) element stiffness matrix. The present study also incorporates the straightforward prediction of interlaminar stresses from equilibrium equations. Several numerical examples confirm the superior behavior of the present composite laminated curved beam element.

Key Words : Composite Laminated Curved Beam Element, Hybrid-Mixed Formulation, Interlaminar Stresses, First-order Shear Deformation Lamination Theory, Stress Parameters, Field Consistency

1. Introduction

Fiber-reinforced composite laminates with high specific stiffness and strength are widely used for lightweight structures. By choosing the fiber orientation in each lamina and stacking sequence of the layers, a number of desired structural as well as thermal characteristics can be designed. The increasing use of composite materials demands clear understanding of their behavior and performance under severe operating environments. A delamination can be caused by the shear stresses between the layers due to the mismatch of material properties between materials. An understanding of failure due to delamination is of considerable importance in the reliable analysis and design of advanced fiber reinforced composite structures.

Beams are the simplest and most commonly used structural elements used in a variety of engineering structures. The earliest attempts to develop a thin curved beam element based on the Kirchhoff-Love theory were not successful when C^0-continuous tangential and C^1-continuous normal displacements are employed (Ashwell and Sabir, 1971 ; Dawe, 1974). Some shear flexible arch elements based on the Mindlin-Reissner theory permit the use of C^0-continuous interpolation functions for displacements (Noor et al., 1977 ; Noor and Peters, 1981 ; Stolarski and Belytschko, 1983). The Mindlin-Reissner theory requires a shear correction factor to correct the strain energy of deformation. Higher order beam theories have been proposed to model the cross-sectional warping and to remove the shear correction factor (Stephen and Levinson, 1979 ; Levinson, 1981a ; Levinson, 1981b ; Rychter, 1987 ; Kant and Manjunath, 1989).

These early attempts were unsuccessful because the developed elements are suffered from an excessive bending stiffness, called membrane lock-

* Corresponding Author,
E-mail : kimjg1@cu.ac.kr
TEL : +82-53-850-2711; **FAX** : +82-53-850-2710
School of Mechanical & Automotive Engineering, Catholic University of Daegu, Hayang-up, Kyongsan-si, Kyongbuk, 712-702, Korea. (Manuscript **Received** August 20, 2004; **Revised** January 20, 2005)

ing, in the limit of inextensional bending or excessive shearing, called shear locking, in the thin-beam limit (Dawe, 1974; Noor et al., 1977; Noor and Peters, 1981; Stolarski and Belytschko, 1983). To alleviate these numerical difficulties, special techniques based on the most popular minimum potential energy principle are proposed, such as the selective/reduced integration technique (Stolarski and Belytschko, 1982; Moon et al., 1996), field-consistent element (Prathap and Babu, 1986) and strain-based element (Ryu and Sin, 1996), etc. Besides these displacement elements, hybrid-mixed finite elements (Saleeb and Chang, 1987; Dorfi and Busby, 1994; Kim and Kim, 1998; Kim, 2000) based on the Hellinger-Reissner variational principle have been shown to be quite successful. Among others, Kim and Kim (1998) propose a new hybrid-mixed curved beam element, which may be the most accurate locking-free curved beam element by introducing the nodeless degrees of freedom and consistent stress parameters.

In this paper, we propose a new hybrid-mixed composite laminated curved beam element with nodeless degrees of freedoms. The introduction of nodeless degrees makes possible to estimate the interlaminar stresses by choosing stress equilibrium equations. The present laminated curved beam element is based on the first-order shear deformation lamination theory. In many problems, the use of stacking sequences, which do not exhibit the transverse deformation to the load plane, makes a two dimensional analysis of curved laminated composite beams practically useful. For the development of the present hybrid-mixed element, the field-consistency concept (Prathap and Babu, 1986; Kim and Kim, 1998) is utilized to select appropriate stress parameters. At the element level, the stress parameters are eliminated from the stationary condition and the nodeless degrees of freedom are also removed by static condensation (Cook et al., 1989) so that a standard six-by-six stiffness matrix is finally obtained. The efficiency of the present element can well compensate the additional computational effort necessary in the element level. The numerical results in several test problems confirm the excellent performance of the present element.

2. Hellinger-Reissner Variational Principle

Fig. 1 shows a two-noded curved beam element with six displacement degrees of freedom. The tangential and transverse displacements are denoted by u and v, the normal rotation, θ. The tangential and transverse stress resultants are defined as N and V, and the moment resultant, M. The corresponding nodal values are subscribed with 1 and 2. The curved beam element has the thickness h, the initial radius of curvature R and the length l.

The Hellinger-Reissner variational principle for an element (Washizu, 1982) is expressed

$$\Pi_R=\int_c\left[-\frac{1}{2}\boldsymbol{\sigma}^t\mathbf{S}\boldsymbol{\sigma}+\boldsymbol{\sigma}^t\boldsymbol{\varepsilon}\right]dx-W \tag{1}$$

where

$$W=\int_c(p_x u+p_y v)\,dx+\sum_{i=1}^{2}(N_i u_i+V_i v_i+M_i\theta_i) \tag{2}$$

In Eqs. (1) and (2), the generalized stress $\boldsymbol{\sigma}$ and strain $\boldsymbol{\varepsilon}$ vectors are defined as $\boldsymbol{\sigma}=[N,\ V,\ M]^t$ and $\boldsymbol{\varepsilon}=[\varepsilon_0,\ \gamma_0,\ \kappa]^t$, respectively. The generalized material compliance matrix is denoted by $\mathbf{S}$. The kinematic relations and constitutive equations are found from the general shell theory by Naghdi and Reissner (Saleeb and Chang, 1987):

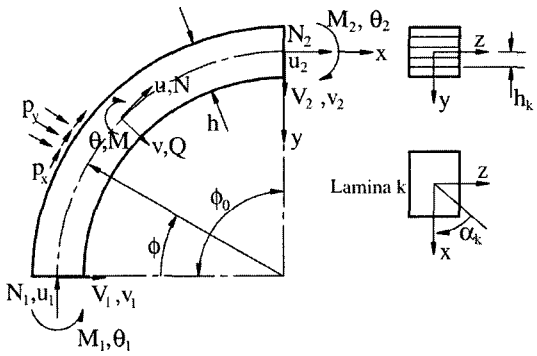

Fig. 1 The geometry of a two-noded curved beam element

$$\varepsilon_0=\frac{1}{R}\frac{du}{d\varphi}-\frac{v}{R}$$
$$\kappa=\frac{1}{R}\frac{d\theta}{d\varphi} \tag{3}$$
$$\gamma_0=\frac{u}{R}+\frac{1}{R}\frac{dv}{d\varphi}-\theta$$

where φ is the circumferential angle. Assuming that $(y/R)^2\ll 1$, the normal and shear strain components ε_x and γ_{xy} for a deep curved beam at a distance y from the reference surface can be denoted by

$$\varepsilon_x=\frac{1}{1-y/R}(\varepsilon_0-y\kappa)\approx\left(1+\frac{y}{R}+\frac{y^2}{R^2}\right)(\varepsilon_0-y\kappa) \tag{4a}$$

$$\gamma_{xy}=\frac{\gamma_0}{1-y/R}\approx\left(1+\frac{y}{R}+\frac{y^2}{R^2}\right)\gamma_0 \tag{4b}$$

For a single ply denoted by k, the stress-strain relations for a two-dimensional beam analysis are

$$\sigma_x^k=E_x^k\varepsilon_x^k \tag{5a}$$

$$\tau_{xy}^k=G_x^k k_s\left[1-\frac{4y^2}{h^2}\right]\gamma_{xy}^k \tag{5b}$$

where E_x^k and G_x^k are the effective elastic modulus and the shear modulus, respectively, and k_s is the shear factor. The thermal and hygrothermal effects and the temperature variation of the elastic constants are not considered in the present formulations. We can express E_x^k and G_x^k from the properties in principal material directions and the angle α_k between the fiber direction and the beam length axis (Vinson and Sierakowski, 1986) as follows.

$$E_x^k=\frac{\cos^4\alpha_k}{E_{11}}+\left(\frac{1}{G_{12}}-\frac{2\nu_{12}}{E_{11}}\right)\cos^2\alpha_k\sin^2\alpha_k+\frac{\sin^4\alpha_k}{E_{22}} \tag{6a}$$

$$G_x^k=G_{13}\cos^2\alpha_k+G_{23}\sin^2\alpha_k \tag{6b}$$

Substituting Eqs. (4) and (5) into the equations for stress resultants and integrating the stress resultants over the cross-sectional area, then we can construct the following matrix form

$$\sigma=\begin{Bmatrix}N\\V\\M\end{Bmatrix}=\begin{Bmatrix}\sum_{k=1}^{NL}\int_{h_{k-1}}^{h_k}\sigma_x^k b\,dy\\ \sum_{k=1}^{NL}\int_{h_{k-1}}^{h_k}\tau_{xy}^k b\,dy\\ \sum_{k=1}^{NL}\int_{h_{k-1}}^{h_k}\sigma_x^k y b\,dy\end{Bmatrix}=\begin{bmatrix}\Gamma_{11}&0&\Gamma_{13}\\0&\Gamma_{22}&0\\\Gamma_{13}&0&\Gamma_{33}\end{bmatrix}\begin{Bmatrix}\varepsilon_0\\\gamma\\\kappa\end{Bmatrix}=\Gamma\cdot\varepsilon \tag{7}$$

where

$$\Gamma_{11}=A_1+\frac{A_2}{R}+\frac{A_3}{R^2} \tag{8a}$$

$$\Gamma_{13}=-\left(A_2+\frac{A_3}{R}+\frac{A_4}{R^2}\right) \tag{8b}$$

$$\Gamma_{22}=k_s\left[B_1+\frac{B_2}{R}+\left(\frac{1}{R^2}-\frac{4}{h^2}\right)B_3-\frac{4B_4}{Rh^2}-\frac{4B_5}{R^2h^2}\right] \tag{8c}$$

$$\Gamma_{33}=A_3+\frac{A_4}{R}+\frac{A_5}{R^2} \tag{8d}$$

In the above, the coefficients are defined as

$$A_n=\sum_{k=1}^{NL}E_x^k b(h_k^n-h_{k-1}^n)/n\quad(n=1,\cdots,5) \tag{9a}$$

$$B_n=\sum_{k=1}^{NL}G_x^k b(h_k^n-h_{k-1}^n)/n\quad(n=1,\cdots,5) \tag{9b}$$

where NL and b denote the number of laminates and the beam width, respectively. The compliance matrix $\mathbf{S}$ needed in Eq. (1) can be obtained from the inverse of the constitutive matrix $\boldsymbol{\Gamma}$ in Eq. (7).

The thickness variation of constitutive laws and continuity requirements across interfaces make the three/two-dimensional finite element analysis very difficult. In addition, a large number of elements are required to gain acceptable levels of accuracy particularly with reference to stress continuity requirements at the interface. For these reasons, Kant and Manjunath (1989) have shown that by integrating the two stress equilibrium equations of two-dimensional elasticity for each layer over the lamina thickness and summing over layer 1 to L, estimates of interlaminar stresses can be obtained as follows.

The differential equations of equilibrium representing the pointwise equilibrium can be written as

$$\tau_{i,j}=0 \quad (i, j=x, y) \tag{10}$$

Substituting of the lamina stress in Eq. (10) and integrating, the interlaminar shear stress can be obtained as

$$\tau_{xy}^{L}|_{y=h_L+1}=-\sum_{k=1}^{L}\int_{h_k}^{h_{k+1}}\frac{\partial\sigma_x}{\partial x}dy+C_1 \tag{11}$$

Substituting the lamina stress in Eq. (10) and eliminating interlaminar shear stress, the following second order differential equation is obtained.

$$\frac{\partial^2\sigma_x}{\partial x^2}=\frac{\partial^2\sigma_y}{\partial y^2} \tag{12}$$

The integration of Eq. (12) yields the following interlaminar normal stress as

$$\sigma_y^{L}|_{y=h_L+1}=-\sum_{k=1}^{L}\int_{h_k}^{h_{k+1}}\left(\int_y\frac{\partial^2\sigma_x}{\partial x^2}dy\right)dy+yC_2+C_3 \tag{13}$$

The constants of integration are so determined to sastisfy the conditions for σ_y and τ_{xy} on $z=\pm h/2$ (Pagano, 1969). In view of availability of only a single constant, the interlaminar shear stress estimate may not in general satisfy beam boundary conditions at the boundary surfaces. In case of interlaminar normal stress, this problem does not arise, because here two constants of integration obtained by integrating twice can be determined by substituting two boundary conditions at $z=\pm h/2$. Eq. (13) is solved as a boundary value problem, but this requires use of at least a cubic element, so that the third derivatives of displacements can be determined. Present element satisfy this requirement.

3. Field Assumption

For the present hybrid-mixed two-noded cubic element, we propose to use bubble functions such as $\xi(1-\xi)$ and $\xi^2(1-\xi)$ in addition to the usual linear interpolation functions for displacements. Using the dimensionless co-ordinate $\xi=\varphi/\varphi_0$ $(0\leq\xi\leq1)$, the following displacement interpolation is considered.

$$\begin{aligned}u&=(1-\xi)u_1+\xi u_2+\xi(1-\xi)a_1+\xi^2(1-\xi)a_2\\ v&=(1-\xi)v_1+\xi v_2+\xi(1-\xi)b_1+\xi^2(1-\xi)b_2\\ \theta&=(1-\xi)\theta_1+\xi\theta_2+\xi(1-\xi)c_1+\xi^2(1-\xi)c_2\end{aligned} \tag{14}$$

one may put equation (14) in compact form

$$\mathbf{u}=[\mathbf{N}_c\,:\,\mathbf{N}_b]\cdot\begin{Bmatrix}\mathbf{d}_c\\ \mathbf{d}_b\end{Bmatrix}=\mathbf{N}\cdot\mathbf{d} \tag{15}$$

where $\mathbf{d}_b=\{a_1, \cdots c_2\}^t$ are the nodeless degrees of freedom which are associated with significant deformation at $\xi=1/2$ with vanishing deformation at nodes, $\xi=0$ and 1. The conventional nodal displacement components are defined by $\mathbf{d}_c=\{u_1, \cdots, \theta_2\}^t$.

To select appropriate stress interpolation functions needed in the hybrid-mixed formulation, the limiting behavior of strains should be examined. As the beam becomes extremely thin and nearly straight, i.e., $(R\rightarrow\infty)$, the shear strain must vanish.

$$\gamma_0=\frac{dv}{l_0 d\xi}-\theta\rightarrow0 \tag{16}$$

Examining equation (16), one sees that four constraints including $c_2\rightarrow0$ are imposed as the shear strain γ_0 approaches zero. In particular, the constraint of vanishing c_2 yields the unnecessary constraint expressed by $\theta_{,\xi\xi\xi}\rightarrow0$ in the element region (Prathap, 1993). Similarly in the limit of inextensional bending, we can find one spurious constraint of vanishing b_2 by examining the limiting behavior of

$$\varepsilon_0=u_{,\xi}+\frac{v}{R}\rightarrow0 \tag{17}$$

Obviously, the consequence of the constraint on b_2 is that the term $v_{,\xi\xi\xi}$ vanishes in the element level. To overcome these spurious constraints, which lead to locking phenomena and stress oscillations over the element, the quadratic stress functions should be adopted as

$$\boldsymbol{\sigma}=\begin{Bmatrix}N\\ V\\ M\end{Bmatrix}=\mathbf{P}\cdot\boldsymbol{\beta} \tag{18}$$

where

$$\boldsymbol{\beta}=(\beta_1\ \beta_2\ \cdots\ \beta_8\ \beta_9)^T \tag{19}$$

and

$$\mathbf{P}=\begin{bmatrix}1&0&0&\xi&0&0&\xi^2&0&0\\ 0&1&0&0&\xi&0&0&\xi^2&0\\ 0&0&1&0&0&\xi&0&0&\xi^2\end{bmatrix} \tag{20}$$

These consistent stress parameters can be reconfirmed by the matching requirement of stress-displacement fields (Pian and Chen, 1983), Dim $(\boldsymbol{\beta}) \geq \text{Dim}(\mathbf{u}) -$ *the number of rigid-body degrees of freedoms*, namely $\text{Dim}(\boldsymbol{\beta}) \geq 12-3=9$. The present consistent higher-order hybrid-mixed curved composite beam element based on Eqs. (15) and (18) will be designated by CDCSQ2. This element will. be compared with 2-noded hybrid-mixed element designated by CDQSL2, which has consistent quadratic displacement-linear stress approximation.

4. Finite Element Formulation

For the finite element formulation, Eqs. (15) and (18) are substituted into Eq. (1) to yield

$$\Pi_R=\boldsymbol{\beta}^t\mathbf{G}\mathbf{d}-\frac{1}{2}\boldsymbol{\beta}^t\mathbf{H}\boldsymbol{\beta}-\mathbf{d}^t\boldsymbol{\phi}-\mathbf{Q}^t\mathbf{d} \tag{21}$$

where

$$\mathbf{H}=\int_c\mathbf{P}^t\mathbf{S}\mathbf{P}\,dx \tag{22}$$

$$\mathbf{G}=\int_c\mathbf{P}^t\mathbf{B}\,dx=\int_c\mathbf{P}^t[\mathbf{B}_c\,:\,\mathbf{B}_b]\,dx=[\mathbf{G}_c\,:\,\mathbf{G}_b] \tag{23}$$

$$\boldsymbol{\phi}=\int_c\mathbf{N}_c^t[p_x,\ p_y,\ 0]\,dx \tag{24}$$

Here, the matrix $\mathbf{G}$ is expressed in terms of the strain-displacement matrix $\mathbf{B}_c$ and $\mathbf{B}_b$ which correspond to the nodal and nodeless displacement components, respectively, and $\boldsymbol{\phi}$ is the consistent load vector due to surface tractions. The applied nodal force vector is also denoted by $\mathbf{Q}$.

Invoking the stationarity of the functional with respect to $\mathbf{d}$ and $\boldsymbol{\beta}$ gives

$$\mathbf{G}^t\boldsymbol{\beta}=\mathbf{Q}+\boldsymbol{\phi} \tag{25a}$$

$$\mathbf{H}^t\boldsymbol{\beta}=\mathbf{G}\mathbf{d} \tag{25b}$$

The elimination of $\boldsymbol{\beta}$ in Eq. (25) in the element level yields the following form of equations:

$$\begin{bmatrix}\mathbf{K}_{cc} & \mathbf{K}_{cb}\\ \mathbf{K}_{bc} & \mathbf{K}_{bb}\end{bmatrix}\begin{Bmatrix}\mathbf{d}_c\\ \mathbf{d}_b\end{Bmatrix}=\begin{Bmatrix}\mathbf{Q}+\boldsymbol{\phi}\\ \mathbf{0}\end{Bmatrix} \tag{26}$$

where the element substiffness matrices $\mathbf{K}_{ij}$ are

$$\mathbf{K}_{ij}=\mathbf{G}_i^t\mathbf{H}^{-1}\mathbf{G}_j \quad (i \text{ and } j=c,\ b) \tag{27}$$

Since the nodeless variables $\mathbf{d}_b$ are designed not to carry any load, $\mathbf{d}_b$ can be eliminated in the element level by the condensation of Eq. (26).

$$\mathbf{d}_b=-\mathbf{K}_{bb}^{-1}\mathbf{K}_{bc}\mathbf{d}_c \tag{28}$$

The substitution of Eq. (28) into the first set of equations in Eq. (26) results in

$$\mathbf{K}^e\cdot\mathbf{d}_c=\mathbf{Q}+\boldsymbol{\phi} \tag{29a}$$

$$\mathbf{K}^e=\mathbf{K}_{cc}-\mathbf{K}_{cb}\mathbf{K}_{bb}^{-1}\mathbf{K}_{bc} \tag{29b}$$

This element stiffness matrix $\mathbf{K}^e$ of a CDCSQ2 element can now be treated easily for the assembly and subsequent analysis. If the constant stress and linear displacement field is employed without the use of nodeless variables, the resulting stiffness, which is equal to $\mathbf{K}_{cc}$, reduces exactly to the stiffness matrix of a CDQSL2 element and Dorfi's P1-type element (Dorfi and Busby, 1994).

5. Numerical Examples

In this section, we evaluate the numerical performance of the present finite element for the several problems. The present results are compared with those reported by existing analytical and/or numerical results.

5.1 Composite cantilever beam bending

To show whether the present element exhibits locking problem for thin beam, a thin composite cantilever beam under the tip load P at the free end is considered since its analytical solution is well known. Material and geometric data are given in Table 1 (Vinson and Sierakowski, 1994). Using the Timoshenko beam theory applied to laminated composites, the tip deflection is given by

$$v_{theory}=PL^3\left[\Gamma_1\left(-\frac{1}{3}\left(\frac{x}{L}\right)^3+\left(\frac{x}{L}\right)^2\right)+\Gamma_2\left(\frac{x}{L}\right)\right]$$

and

$$\Gamma_1=\frac{A_1}{2(A_1A_3-A_2^2)}\,;\ \Gamma_2=\frac{1}{k_s(B_1-4B_3/h^2)}$$

where L is the length of the beam, h the thickness of the beam, k_s the shear factor and (A_1, A_2, A_3, B_1, B_3) are defined by Eq. (9).

Table 1 Material and geometric data of a straight beam

Material (Kevlar epoxy)	
E11	76 GPa
E22	5.5 GPa
G11=G13=G23	2.3 GPa
v_{12}	0.34
Geometry	
Stacking sequence	[90/45/-45/45/-45/0]s
Beam length	0.5 m
Beam height	12 mm
Beam width	20 mm
Tip transverse load	1 N

Table 2 Material and geometric data of a pinched ring

Material (graphite epoxy)	
E_{11}	289 GPa
E_{22}	6.06 GPa
$G_{12}=G_{13}=G_{23}$	4.13 GPa
v_{12}	0.31
Geometry	
Stacking sequence	[90/45/-45/45/-45]s
Radius R	0.1 m
Beam height h	20 mm
Beam width b	20 mm
Shear factor k_s	1.2

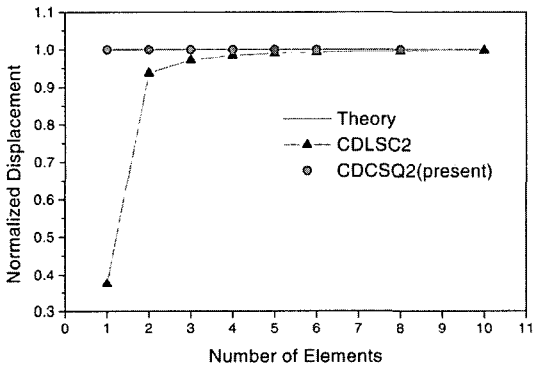

Fig. 2 Convergence behavior of the normalized displacement at the loaded point in the straight cantilever beam

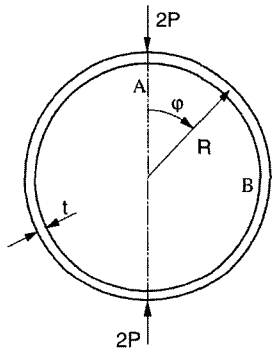

Fig. 3 Composite ring under compressive point load

Figure 2 shows the convergence behavior for the normalized tip deflection at the free edge. It is clear that the CDCSQ2 element shows more rapid convergence than the CDQSL2 element. The CDCSQ2 element requires some additional calculations to obtain $\mathbf{K}_{cb}\mathbf{K}_{bb}^{-1}\mathbf{K}_{bc}$ in Eq. (29b) for each element. Regardless of the additional computational effort needed for CDCSQ2, CDCSQ2 with the additional nodeless degrees is more effective than CDQSL2.

5.2 Composite pinched ring

Figure 3 shows a composite pinched ring with a radius of 0.1 m and thickness of 0.02 m ($R/h=5$) subjected to compressive point loads in radial direction. A pinched ring serves as the best illustration to evaluate the element behavior in a deep arch problem. The quadrant from A to B of the ring is modeled because of the double symmetry. Material and geometric data are given in Table 2 (Vinson and Sierakowski, 1994).

The convergence behavior of present element is demonstrated in Fig. 4. It is seen that the CDCSQ2 element gives more rapidly converging results than the CDQSL2 element without nodeless degrees. To compare the performance of CDCSQ2 and CDQL2 in the stress prediction, the normal force distributions obtained from the various subdivision are plotted in Fig. 5. The accurate prediction of the generalized stresses is very important for the subsequent calculation of the interlaminar stresses to cause a delamination. We can see that the two element idealization with CDCSQ2 yields the results excellently agreeing

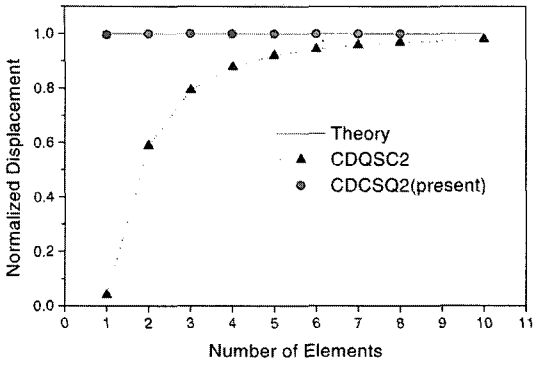

Fig. 4 Convergence of the normalized radial displacement at the loaded point in the pinched ring shown in Fig. 3

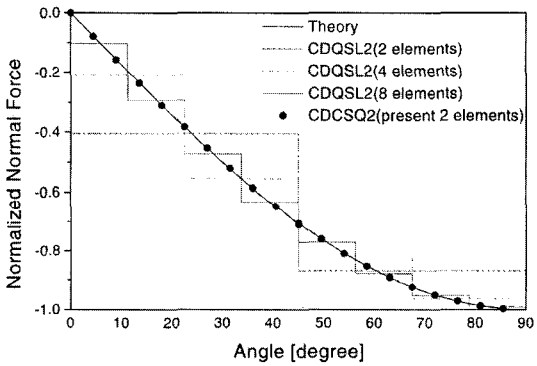

Fig. 5 Normal force approximation of the composite pinched ring

with the exact theoretical normal force distribution $N=-P\sin\varphi$.

5.3 Simply-supported beam under sinusoidal transverse load

Figure 6 shows a simply-supported beam under sinusoidal transverse load $p_y=p_0\sin(\pi x/L)$. In order to compare the present result with those by the elasticity theory and the classical laminated plate theory(CPT) given by Pagano (1969), we consider layers of square symmetric unidirectional fibrous composite material possessing the following stiffness properties in Table 3, which simulate a high modulus graphite/epoxy composite. Subscripts L and T denote the direction parallel to the fibers and the transverse direction, respectively. The geometrical configuration is a symmetric 3-ply laminate with layers of equal

Table 3 Material data of a simply-supported beam

Material (graphite/epoxy)	
E_L	25,000 ksi
E_T	1,000 ksi
G_{LT}	500 ksi
G_{TT}	200 ksi
$\upsilon_{LT}=\upsilon_{TT}$	0.25

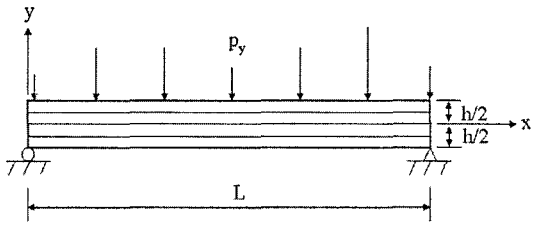

Fig. 6 Simply-supported beam under sinusoidal transverse load

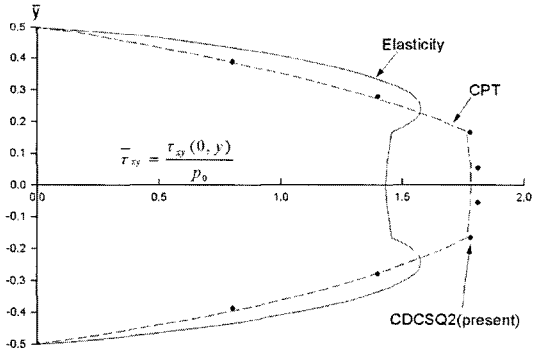

Fig. 7 Thickness vs interlaminar shear stress

thickness - the L direction coincides with x in the outer layers, while T is parallel to x in the central layer. A shear correction factor of 1.2 and a span-to-depth ratio of 4 are used in this study.

The distributions of the normalized interlaminar shear stress $\bar{\tau}_{xy}$ and the normalized in-plane stress $\bar{\sigma}_x$ are shown in Fig. 7 and Fig. 8, respectively. The present results for $\bar{\tau}_{xy}$ and $\bar{\sigma}_x$ substantially agree with the CPT solution by Pagano. Finally, the distribution of the normalized interlaminar normal stress $\bar{\sigma}_y$ is shown in Fig. 9. The distribution of interlaminar normal stress integrating twice the second derivatives of σ_x slightly underestimates the value compared to

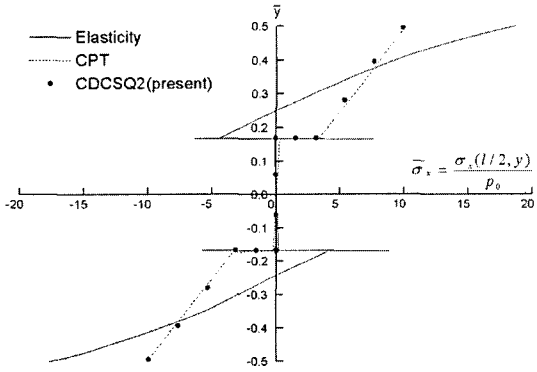

Fig. 8 Thickness vs in-plane stress

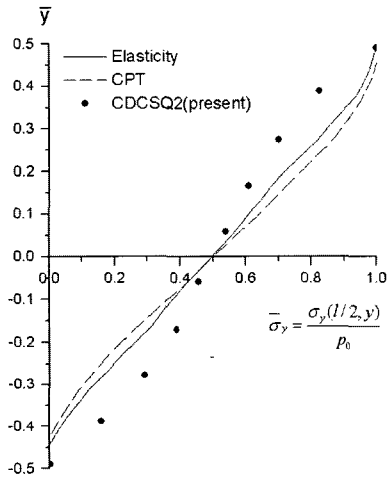

Fig. 9 Thickness vs interlaminar normal stress

the elasticity solution near the top surface of the beam. Although additional computational efforts on the element level are necessary in the present element CDCSQ2, this is well compensated by the increased accuracy and the practical prediction of the interlaminar stresses.

6. Conclusions

In this work, we propose a new highly accurate hybrid-mixed laminated curved beam element introducing the nodeless degrees, which can handle the prediction of interlaminar stress by choosing stress equilibrium equations. The present laminated curved beam element, which is based on the Hellinger-Reissner variational principle and the first-order shear deformation lamination theory, employs consistent stress parameters corresponding to cubic displacement polynomials to resolve the numerical difficulties due to the spurious constraints and improve the accuracy. The stress parameters are eliminated and the nodeless degrees are condensed out to obtain the conventional element stiffness matrix. Several numerical examples confirm the accuracy and efficiency of the present hybrid-mixed laminated curved beam element.

References

Ashwell, D. G. and Sabir, A. B., 1971, "Limitations of Certain Curved Beam Elements When Applied to Arches," *Internat. J. Mech. Sci.*, Vol. 13, pp. 133~139.

Cook, R. D., Malkus, D. S. and Plesha, M. E., 1989, *Concepts and Applications of Finite Element Analysis*, 3rd Edition, Wiely, New York.

Dawe, D. J., 1974, "Numerical Studies Using Circular Arch Finite Elements," *Computers & Structures*, Vol. 4, pp. 729~740.

Dorfi, H. R. and Busby, H. R., 1994, "An Effective Curved Composite Beam Finite Element Based on the Hybrid-Mixed Formulation," *Computers & Structures*, Vol. 53, pp. 43~52.

Kant, T. and Manjunath, B. S., 1989, "Refined Theories for Composite and Sandwich Beams with C^0 Finite Elements," *Computers & Structures*, Vol. 33, No. 3, pp. 755~764.

Kim, J. G. and Kim, Y. Y., 1998, "A New Higher-Order Hybrid-Mixed Curved Beam Element," *International Journal for Numerical Methods in Engineering*, Vol. 43, pp. 925~940.

Kim, J. G. and Kang, S. W., 2003, "A New and Efficient C^0 Laminated Curved Beam Element," *Transactions of the KSME*, A, Vol. 27, No. 4, pp. 559~ 566.

Kim, J. G., 2000, "Optimal Interpolation Functions of 2-Node Hybrid-Mixed Curved Beam Element," *Transactions of the KSME*, A, Vol. 24, No. 12, pp. 3003~3009.

Levinson, M., 1981, "A New Rectangular beam theory," *Journal of Sound and Vibration*, Vol. 74, pp. 81~87.

Levinson, M., 1981, "Further Results of a New Beam Theory," *Journal of Sound and Vibration*,

Vol. 77, pp. 440~444.

Moon, W. J., Kim, Y. W., Min, O. K. and Lee, K. W., 1996, "Reduced Minimization Theory in Skew Beam Element," *Transactions of the KSME*, Vol. 20, No. 12, pp. 3702~3803.

Noor, A. K. and Peters, J. M., 1981, "Mixed Models and Reduced/Selective Integration Displacement Models for Nonlinear Analysis of Curved Beams," *International Journal for Numerical Methods in Engineering*, Vol. 17, pp. 615~631.

Pagano, N. J., 1969, "Exact Solutions for Composite Laminates in Cylindrical Bending," *Journal of Composite Materials*, Vol. 3, pp. 398~411.

Pian, T. H. H. and Chen, D., 1983, "On the Suppression of Zero Energy Deformation Modes," *International Journal for Numerical Methods in Engineering*, Vol. 19, pp. 1741~1752.

Prathap, G. and Babu, C. Ramesh, 1986, "An Isoparametric Quadratic Thick Curved Beam Element," *International Journal for Numerical Methods in Engineering*, Vol. 23, pp. 1583~1600.

Prathap, G., 1993, *The Finite Element Method in Structural Mechanics*, Kluwer, Dordrecht.

Rychter, Z., 1987, "On the Accuracy of a Beam Theory," *Mechanics Research Communications*, Vol. 14, pp. 99~105.

Ryu, H. S. and Sin, H. C., 1996, "A 2-Node Strain B ased Curved Beam Element," *Transactions of the KSME*, A, Vol. 18, No. 8, pp. 2540~2545.

Saleeb, A. F. and Chang, T. Y., 1987, "On the Hybrid-Mixed Formulation C^0 Curved Beam Elements," *Computer Methods in Applied Mechanics and Engineering*, Vol. 60, pp. 95~121.

Stephen, N. G. and Levinson, M., 1979, "A Second Order Beam Theory," *Journal of Sound and Vibration*, Vol. 67, pp. 293~305.

Stolarski, H. and Belytschko, T., 1983, "Shear and Membrane Locking in Curved Elements," *Computer Methods in Applied Mechanics and Engineering*, Vol. 41, pp. 279~296.

Stolarski, H. and Belytschko, T., 1982, "Membrane Locking and Reduced Integration for Curved Elements," *Journal of Applied Mechanics*, Vol. 49, pp. 172~176.

Vinson, J. R. and Sierakowski, R. L., 1986, *The Behavior of Structures Composed of Composite Materials*, Martinus Nijhoff, Dordrecht.

Washizu, W., 1986, *Variational Methods in Elasticity and Plasticity*, 3rd Ed., Pergamon Press, Oxford.